Seasonal patterns and diagnostic values of δ^2H, $\delta^{18}O$, d-excess, and $\Delta'^{17}O$ in precipitation over Seoul, South Korea (2016–2020)

Songyi Kim[1,2], Yeongcheol Han[2], Hyejung Jung[1], Jeonghoon Lee[1]

[1]Department of Science Education, Ewha Womans University, Seoul, 03760, Republic of Korea
[2]Division of Glacier & Earth Sciences, Incheon, 21190, Korea Polar Research Institute, Republic of Korea

Correspondence to: Jeonghoon Lee (jeonghoon.d.lee@gmail.com)

Abstract. Precipitation stable isotopes are critical tracers for understanding climate variability and the hydrological cycle, as they enable the tracing of moisture sources, air mass mixing, and evaporation vs. condensation mechanisms. In mid-latitude regions such as South Korea, which are influenced by tropical and extratropical circulation, long-term isotope records remain scarce. Here, we analyze stable isotopes in precipitation collected bi-weekly in Seoul, South Korea, from 2016 to 2020. The oxygen isotope composition ($\delta^{18}O$) ranged widely from 1.15 to –18.21‰, hydrogen isotope composition (δ^2H) varied from 3.3 to –132.0‰, the deuterium excess (d-excess) ranged from 23.7 to 2.1‰ and the ^{17}O-excess ($\Delta'^{17}O$) ranged from 69 to –28 per meg. All three primary isotopes exhibited a coherent sinusoidal seasonal cycle, with the most depleted values in winter, gradual enrichment through spring, and sharp depletion during the summer monsoon, reflecting the combined influence of temperature and the amount effect. The d-excess was highest during cold, dry months and lowest in humid, rainy months, reflecting shifts in near-surface relative humidity at the moisture source region and associated kinetic fractionation. Meanwhile, $\Delta'^{17}O$ exhibited a similar season trend with a smaller amplitude, indicating a reduced sensitivity to seasonal variations in relative humidity compared to d-excess and suggesting additional modulation by large-scale transport and water vapor mixing. The local meteoric water line closely matches the global line but winter samples show a higher intercept and a slightly steeper $\delta^{17}O$–$\delta^{18}O$ slope, suggesting enhanced kinetic fractionation under continental air masses. A consistently negative $\delta^{18}O$–$\Delta'^{17}O$ relationship was observed except in winter when it weakened. This integrated analysis of $\delta^{18}O$, d-excess, and $\Delta'^{17}O$ provides a comprehensive picture of source humidity, transport dynamics, and seasonal precipitation processed in a mid-latitude East Asia, and offers a valuable reference for refining isotope-enabled climate models over East Asia.

1 Introduction

Global climate change is modifying the hydrological cycle and increased the frequency of extreme weather events such as droughts and floods (Masson-Delmotte et al., 2021; Trenberth, 2011). In particular, Asia has experienced substantial changes in precipitation intensity and distribution over recent decades, coinciding with continuous surface temperature rise (Masson-Delmotte et al., 2021). Therefore, understanding precipitation processes, which form a critical link between the climate system and water resource management (Masson-Delmotte et al., 2021; Trenberth, 2011), is essential. In this context, stable isotopes ($\delta^{18}O$ and $\delta^{2}H$) in precipitation have emerged as powerful tracers of atmospheric water cycling and climate dynamics (Araguás-Araguás et al., 1998; Craig, 1961; Craig and Gordon, 1965; Dansgaard, 1964; Gat, 1996). In recent years, high-resolution isotope datasets have been increasingly recognized for understanding precipitation characteristics and isotopic responses in East Asia, as they are sensitive to isotopic fractionation during phase changes such as evaporation, condensation, and precipitation formation (Bowen et al., 2018; Cappa et al., 2003; Conroy et al., 2016; Craig and Gordon, 1965; Gat, 1996; Majoube, 1971).

Heavier isotopes (^{18}O and ^{2}H) are preferentially removed from atmospheric water vapor during condensation and precipitation formation and enriched during evaporation and sub-cloud re-evaporation, with the strength of this fractionation varies with environmental parameters such as temperature, relative humidity, and precipitation amount (Conroy et al., 2016; Craig and Gordon, 1965; Gat, 1996). Two well-known relationships, the temperature effect, where colder temperatures lead to lower $\delta^{18}O$ and $\delta^{2}H$ values, and the amount effect, where increased rainfall results in isotope depletion of stable water isotope, have been widely observed in various climate regimes (Araguás-Araguás et al., 1998; Dansgaard, 1964). These relationships have established $\delta^{18}O$ and $\delta^{2}H$ as powerful diagnostic tools for hydrological and climatological studies, as well as paleoclimate reconstructions (Jouzel et al., 1997; Winkler et al., 2012). However, the stable isotopic composition of precipitation ($\delta^{18}O$ and $\delta^{2}H$) is governed by both equilibrium and kinetic fractionation during phase changes such as evaporation and condensation, making it difficult to isolate the relative contributions of each process. In addition to $\delta^{18}O$ and $\delta^{2}H$, recent analytical advances have enabled high-precision measurements of $\delta^{17}O$. Under both equilibrium and kinetic fractionation, $\delta^{17}O$ and $\delta^{18}O$ follow mass-dependent fractionation relationships, but with distinct slopes. Simultaneous measurement of $\delta^{17}O$ and $\delta^{18}O$, therefore, enables the quantification of subtle deviations from the equilibrium reference relationship, forming the basis of triple oxygen isotope ($\delta^{17}O$ and $\delta^{18}O$) studies (Angert et al., 2004; Luz and Barkan, 2010). Secondary parameters, namely deuterium excess (d-excess; $d-excess(‰) = \delta\,^{2}H - 8 \times \delta^{18}O$; defined by Dansgaard, 1964) and ^{17}O-excess ($\Delta'^{17}O$; $\Delta'^{17}O = \ln\left(\delta^{17}O + 1\right) - 0.528 \times \ln\left(\delta^{18}O + 1\right)$; defined by Luz and Barkan, 2010) are primarily sensitive to kinetic fractionation processes and thus help to disentangle them. While $\delta^{18}O$ and $\delta^{2}H$ mainly record equilibrium fractionation, d-excess and ^{17}O-excess reflect deviations from equilibrium associated with non-steady-state evaporation driven by humidity gradients, as well as water vapor mixing or supersaturation during cloud formation (Gat, 1996; Uemura et al., 2008). In contrast to d-excess, which is primarily sensitive to relative humidity at the moisture source, $\Delta'^{17}O$, defined as the logarithmic deviation from the

mass-dependent reference relationship between $\delta^{17}O$ and $\delta^{18}O$, is less directly controlled by humidity and more sensitive to non-equilibrium processes such as large-scale water vapor mixing and supersaturated condensation, thereby providing complementary information on the dynamical history of atmospheric moisture (Barkan and Luz, 2007; Benetti et al., 2014; Landais et al., 2008). Recent analytical advances have enabled high-precision $\Delta'^{17}O$ measurements, making this parameter a promising tracer of kinetic isotopic effects in the atmosphere. However, observational datasets for $\Delta'^{17}O$ remain scarce in mid-latitude East Asia, and few studies have explored its co-variability with d-excess in this region. This study addresses these gaps by analyzing d-excess and $\Delta'^{17}O$ in mid-latitude precipitation to better constrain the seasonal behavior and origin of precipitation over the Korean Peninsula.

Mid-latitude regions, such as the Korean Peninsula, exemplify the complex climatic controls on precipitation isotopes (Ha et al., 2012; Huang et al., 2007; Kim et al., 2019; J. Lee et al., 2013, K. Lee et al., 2003). The peninsula lies at the convergence between extratropical westerlies and the East Asian monsoon, resulting in large seasonal differences in moisture sources. In summer, moisture-rich air masses from subtropical oceans (e.g., the western North Pacific) dominate, bringing heavy monsoonal rainfall. This often yields an amount-effect signal where $\delta^{18}O$ values decrease during periods of high precipitation. In contrast, winter precipitation is dominated by cold, dry continental air from the Siberian-Mongolian High, which acquires limited moisture while crossing the Yellow Sea. As a result, winter precipitation is typically more $\delta^{18}O$-depleted due to the lower temperatures and higher upstream rainout. These seasonal contrasts produce a strong annual cycle in precipitation isotope composition in the region, which is highly diagnostic of monsoon strength, moisture source changes, and temperature variability. Accordingly, long-term changes in precipitation isotopes (e.g., $\delta^{18}O$, $\delta^{2}H$, and $\Delta'^{17}O$) may indicate broader hydrological and climatic changes. $\Delta'^{17}O$ measurements offer additional diagnostic value as they are largely temperature-independent, reflecting kinetic fractionation sensitive to the relative humidity at the moisture source, for example, changes occurring during water vapor formation or moisture recycling processes (Landais et al., 2008; Luz and Barkan, 2010). This makes $\Delta'^{17}O$ a powerful complementary tracer for detecting subtle changes in atmospheric circulation and regional hydrological processes.

Despite their importance, long-term records of precipitation isotopes over the Korean Peninsula remain limited. The Global Network for Isotopes in Precipitation (GNIP), established in the 1960s, provides baseline data at a global scale; however, its coverage in East Asia is sparse and often discontinuous (Aggarwal et al., 2010). This lack of high-resolution, continuous isotope data limits the understanding of hydrological processes in the Korean Peninsula and their response to climate variability and change. To address this, in this study, a high-temporal-resolution, 5-year record of monthly triple oxygen and hydrogen isotopes in precipitation was obtained over the Korean Peninsula to investigate their seasonal and interannual variability in this mid-latitude setting. The results of this study provide a foundation for investigating moisture source dynamics, the behavior of isotope tracers such as d-excess and $\Delta'^{17}O$, and the long-term isotopic response to climate variability in East Asia. These data are also essential for evaluating isotope-enabled climate models and interpreting regional paleoclimate proxies, and could

accordingly enhance the understanding of hydroclimatic processes in monsoon-affected regions. By employing high-resolution, ground-based isotope observations, this study provides a critical step toward refining the interpretation of atmospheric processes in mid-latitude monsoon-affected regions.

2 Study area and methods

The measurements were made approximately 30 km inland from the western coast of the Korean Peninsula, on the campus of Ewha Womans University in Seoul, South Korea (37°33'53" N, 126°56'46" E; Fig. 1A and B). The sampling point was located 80 m above sea level. The study area experiences a temperate monsoon climate, with large seasonal variations characterized by hot, humid summers driven by the East Asian summer monsoon and cold, dry winters dominated by the Siberian High and the East Asian winter monsoon (Kim et al., 2019; Lee et al., 2013). The Korean Peninsula experiences a temperate monsoon climate with four distinct seasons, spring (March–May; MAM), summer (June–August; JJA), autumn (September–November; SON), and winter (December–February; DJF) (Ha et al., 2012; Lee et al., 2013). In summer, moist southwesterly winds bring heavy rainfall associated with the East Asian monsoon front, known regionally as the *Changma* in Korea peninsula, *Meiyu* in China, and *Baiu* in Japan, resulting in the concentration of annual precipitation within a few months. In winter, the strengthening of the extensive Siberian High pushes cold, dry air southward across the peninsula (Ding and Chan, 2005). Spring is generally mild and dry, whereas autumn is cooler and occasionally affected by typhoons or tropical storms that deliver intense rainfall events.

Precipitation samples were collected between January 2016 and December 2020 (five years) at approximately biweekly intervals. For each collection period, the deployment bottle remained in placed to accumulate all precipitation events within the interval. No mineral oil was applied to prevent evaporation during precipitation collection, because the presence of organic compounds can interfere with spectroscopic isotope analysis in cavity ring-down systems. Previous studies have demonstrated that even trace amounts of organic contamination, such as mineral oil residues, can cause spectral interference and bias δ^2H and $\delta^{18}O$ measurements obtained by WS-CRDS (Gupta et al., 2009). Instead of using oil, we employed a funnel system that physically minimized post-collection evaporation. Precipitation was funneled directly into pre-cleaned and sealed PTFE bottles immediately after sampling period, thereby minimizing exposure to air and sunlight. Samples were collected on an unobstructed rooftop of a five-story building. This point was selected because its open setting, free from nearby buildings or vegetation, ensured that the collected precipitation was representative and minimally affected by local interference (Fig. 1C). All precipitation samples were stored in pre-cleaned HDPE bottles and sealed with Parafilm, and were kept frozen at −20 °C until preparation for analysis. Before isotope analysis, the samples were thawed, transferred to glass vials, and stored at 4 °C in liquid form for less than two weeks prior to measurement.

All samples were transported in a frozen state to the Korea Polar Research Institute (KOPRI), where water isotope analysis was conducted using a wavelength-scanned cavity ring-down spectrometer (WS-CRDS; model L2140-I, Picarro Inc.,

CA, USA). The analytical protocol followed the optimized method of Kim et al. (2022) for high-precision triple oxygen isotope measurements. For each sample and reference material, duplicate vials were prepared; the first vial was discarded to eliminate memory and carryover effects, and only the final six injections from the second vial were averaged for analysis. This strategy significantly reduced memory effects associated with isotopic differences between successive samples, and three international reference waters (Vienna Standard Mean Ocean Water (VSMOW), Standard Light Antarctic Precipitation (SLAP), and Greenland Ice Sheet Precipitation (GISP)), together with one in-house standard, were used for normalization to the VSMOW–SLAP scale. At the beginning of each analytical session, international reference waters (VSMOW2, SLAP2, and GISP) were measured for VSMOW–SLAP scale normalization. Subsequently, samples were analyzed, and every ten samples, two in-house laboratory standards (STYX and KT), both calibrated against VSMOW2 and SLAP2, were analyzed to monitor instrumental performance. STYX, a natural water collected from the Styx Glacier region in Antarctica, was used to assess the long-term analytical reproducibility of the WS-CRDS, while KT, a locally sourced tap water with isotopic composition similar to the precipitation samples, was used to reduce potential memory effects during analysis. The long-term 1σ standard deviations obtained from repeated STYX measurements over several years were ±0.10‰ for δ^2H, ±0.07‰ for $\delta^{18}O$, and ±0.01‰ for $\delta^{17}O$, while the 1-year reproducibility for $\Delta'^{17}O$ was ±9 per meg (Kim et al., 2022). All data were reported relative to VSMOW using the delta notation (δ) (Eq. (1)):

$$\delta(‰) = \left(\frac{R_{sample}}{R_{VSMOW}} - 1\right) \times 1000, \quad (1)$$

where R_{sample} and R_{VSMOW} represent the isotopic ratios of the sample (i.e., $^{18}O/^{16}O$, $^{17}O/^{16}O$, or $^{2}H/^{1}H$) and VSMOW, respectively.

To account for multiple precipitation events within a month, precipitation-weighted monthly means (δ_{wm}) were calculated for δ^2H, $\delta^{18}O$, and $\delta^{17}O$ as follows (Eq. (2)):

$$\delta_{wm} = \frac{\sum P_i \times \delta_i}{\sum P_i} \quad (2)$$

where P_i is the precipitation amount and δ_i is the isotopic value for each event. Although precipitation samples were collected at approximately 14-day intervals, all seasonal and intermonthly analyses in this study are based on precipitation-weighted monthly mean values. For months with two biweekly samples, the isotope values were weighted by their corresponding precipitation amounts to derive monthly means (δ_{wm}).

Meteorological data, including air temperature, relative humidity, and precipitation amount, were obtained from hourly observations at the Seoul station operated by the Korea Meteorological Administration (KMA, 2024). For each biweekly sampling interval, the hourly data corresponding to periods with precipitation were integrated to derive time-weighted mean temperature and humidity and cumulative precipitation, representing the meteorological conditions relevant to each collected

sample. The average monthly precipitation amount (grey bars) and average monthly temperature (black-lined boxes) for Seoul, based on these KMA data, are shown in Fig. 2.

3 Results and Discussion

3.1 Variations in precipitation stable isotopes

A total of 130 precipitation samples were collected during the study period. Precipitation-weighted monthly mean values were calculated from the biweekly samples and used for all subsequent analyses. The measured isotopic compositions of precipitation varied considerably: $\delta^{17}O$ ranged from –0.89 to –7.53‰ (average: –3.74‰); $\delta^{18}O$ from –1.74 to –14.25‰ (average: –7.11‰); and $\delta^{2}H$ from –11.8 to –93.5‰ (average: –45.2‰). The d-excess fluctuated between 23.7 and 2.1‰ (average: 11.7‰), whereas $\Delta'^{17}O$ ranged from 56 to –10 per meg (average: 18 per meg). Unlike d-excess, which peaked in winter (median ≈ 17‰) and reached its lowest values in summer (median ≈ 6‰), $\Delta'^{17}O$ displayed a distinct seasonal pattern, being highest in spring (up to ≈ 40 per meg) and lowest in summer (down to ≈ 10 per meg). For all three parameters ($\delta^{17}O$, $\delta^{18}O$ and $\delta^{2}H$), the precipitation isotopic values were relatively depleted during the coldest months (December to February), increased between around March and April as condition warmed, and then sharply decreased between June and August, when precipitation peaked (Fig. 3). This pattern indicates that seasonal variations in $\delta^{18}O$ and $\delta^{2}H$ reflect both temperature-dependent equilibrium fractionation, which dominates during colder periods, and rainfall intensity (amount effect), which lowers $\delta^{18}O$ and $\delta^{2}H$ during intense summer precipitation. The monthly isotopic patterns observed during the study period align with those reported for Jeju Island in the Korean Peninsula and the Yangtze River region in China (Gou et al., 2022; Shin et al., 2021), suggesting that these regions may be influenced by similar meteorological patterns over East Asia. A distinct seasonal variation in d-excess is evident from the box plots (Fig. 3), with higher values in winter (particularly January and February; whole winter median values of 15–20‰) and lower values in summer (medians: 0–5‰). This pattern is consistent with previous findings in the Korean Peninsula and reflects the sensitivity of d-excess to relative humidity and non-equilibrium fractionation processes driven by moisture-source conditions (Kim et al., 2019; Lee and Kim, 2007). In winter, cold, dry air and a steep temperature/humidity gradient between the atmosphere and the ocean (or other moisture sources) enhance evaporation-driven fractionation, thereby elevating d-excess. Conversely, in summer, high relative humidity at the oceanic moisture source reduces kinetic fractionation during evaporation, resulting in lower d-excess values in the source water vapor, while abundant local precipitation and humid conditions further suppress sub-cloud evaporation, collectively leading to substantially lower d-excess in precipitation. This contrast indicates that $\Delta'^{17}O$ and d-excess are influenced by different kinetic fractionation processes operating under distinct seasonal humidity regimes. Overall, the sine fit of the average monthly $\Delta'^{17}O$ values (R^2 =0.53) supports the presence of a coherent seasonal cycle; although not perfectly periodic, $\Delta'^{17}O$ peaks in winter to early spring and reaches a minimum in summer.

3.2 Local Meteoric Water Line

The linear relationship between the precipitation $\delta^{18}O$ and $\delta^{2}H$ defines a Local Meteoric Water Line (LMWL) that closely aligns with the Global Meteoric Water Line (GMWL; Craig, 1961), while exhibiting additional seasonal variations (Fig. 4). The LMWL derived from linear regression is $\delta^{2}H = 7.79 \pm 0.35 \cdot \delta^{18}O + 10.2 \pm 2.7$ ($R^2 = 0.92$, $p < 0.01$), indicating that the isotopic composition of precipitation in Seoul follows the global meteoric trend that reflects equilibrium fractionation on average, although substantial seasonal variations in d-excess demonstrate the coexistence of kinetic effects that partially compensate in the annual regression. The near-identical slope to the GMWL suggests minimal deviation from global meteoric trends, although seasonal changes in moisture sources and humidity may introduce modest variation. Further examination of seasonal subsets revealed distinct differences in isotopic behavior across the year. Summer precipitation clusters tightly along the GMWL, indicating near-equilibrium condensation under humid monsoonal conditions. This pattern is consistent with the dominance of moisture originating from the Northwest Pacific and South China Sea, where high humidity minimizes kinetic fractionation effects. Conversely, winter precipitation plots above the GMWL, with a higher intercept (~20) compared to summer, reflecting the influence of cold, dry air masses and enhanced d-excess.

This difference between summer and winter precipitation suggests that kinetic fractionation, likely associated with ice-phase microphysics and dry air mass transport from the Asian continent, plays a greater role in winter precipitation compared to summer (Kim et al., 2019; Merlivat and Jouzel, 1979; Uemura et al., 2008). Spring and autumn values fall between these seasonal extremes, maintaining an overall LMWL slope close to 8. The persistence of a near-global slope across seasons suggests an apparent equilibrium-like isotopic behavior that may result from either dominant equilibrium fractionation or compensating seasonal kinetic effects, while seasonal intercept variations reflect changes in humidity and moisture source conditions. However, modest seasonal variations in intercept reflect differences in humidity and the moisture source over the year. These findings align with previous studies conducted in Korea based on year-long precipitation isotope records from Chunju, Chuncheon, Jeju, Hongseung and Busan, which reported LMWL slopes ranging from 6.7 to 8.4 and intercepts from 7.7 to 19.2 (Lee et al., 2003; Lim et al., 2012; Shin et al., 2021; Yoon and Koh, 2021). Compared to these, the LMWL in this study shows a similar slope but a slightly lower intercept. This confirms that, while Korean precipitation follows global meteoric trends, seasonal shifts in air mass origin and fractionation processes introduce predictable deviations from these trends (Lee et al., 2007; Lim et al., 2012; Shin et al., 2021; Yoon and Koh, 2021).

The relationship between $\delta'^{17}O$ and $\delta'^{18}O$ in natural waters is generally linear under both equilibrium and kinetic fractionation, but characterized by distinct mass-dependent slopes, with equilibrium fractionation defining the near-global reference slope (Angert et al., 2004; Landais et al., 2008; Luz and Barkan, 2011). This relationship is a fundamental characteristic of stable oxygen isotopes in precipitation, with minor deviations due to kinetic effects, ice-phase processes, and variations in relative humidity at the moisture source (Barkan and Luz, 2005). In the present study, the relationship between precipitation $\delta^{17}O$ and $\delta^{18}O$ defines an LMWL, exhibiting strong linearity across all samples, although including seasonal

variability (Supplementary Table 1). A linear regression applied to the full dataset results in $\delta'^{17}O = 0.528 \pm 0.0010 \times \delta'^{18}O + 0.0208 \pm 0.007$ ($R^2 = 1.00$), confirming the strong linear correlation between $\delta'^{17}O$ and $\delta'^{18}O$ characteristic of mass-dependent fractionation in meteoric waters. A distinct separation in slope occurs when precipitation is classified into winter and non-winter periods. The apparent slope differences in winter precipitation likely reflect the combined influence of equilibrium fractionation, kinetic effects under cold and dry conditions, and additional processes such as water vapor mixing, rather than kinetic fractionation alone (Luz and Barkan, 2011). In this season, Rayleigh distillation along moisture transport pathways further depletes heavy isotopes in precipitation, increasing the $\delta'^{17}O$ and $\delta'^{18}O$ slope, a pattern also observed in high-latitude precipitation (Landais et al., 2012). Ice-phase microphysical processes, particularly supersaturation with respect to ice, cause additional fractionation, reinforcing the seasonal difference in the slope of $\delta^{17}O$ vs $\delta^{18}O$ regression line (Luz and Barkan, 2010). In contrast, non-winter precipitation follows near-equilibrium fractionation, with high humidity minimizing kinetic effects and maintaining $\delta'^{17}O$–$\delta'^{18}O$ ratios similar to those of global meteoric waters (Angert et al., 2004; Landais et al., 2008). These seasonal variations highlight the role of atmospheric humidity and cloud microphysics in modulating triple oxygen isotope fractionation.

The $\delta'^{17}O$–$\delta'^{18}O$ regression derived from the Seoul dataset ($\delta'^{17}O = 0.528 \pm 0.0010 \times \delta'^{18}O + 0.0208 \pm 0.007$; $R^2 = 1.00$) is consistent with results from a nearby GNIP station at Cheongju (~100 km south), which reported $\delta'^{17}O = 0.5283 \times \delta'^{18}O + 0.0216$ (Terzer-Wassmuth et al., 2023). Both stations exhibit nearly identical slopes, and the intercept difference between the two sites is very small (approximately 0.8 per meg), suggesting that local climatic influences on the $\delta'^{17}O$–$\delta'^{18}O$ relationship are limited. This small offset lies within the regional variability observed across East Asia, supporting the interpretation that both datasets reflect the same large-scale atmospheric processes. Taken together, the Seoul record displays an LMWL slope consistent with global meteoric trends while its intercepts and the triple-oxygen isotope relationship align closely with nearby GNIP observations. This coherence demonstrates that the isotopic variability observed in Seoul is regionally representative and largely influenced by seasonal changes in humidity, moisture-source origin, and kinetic fractionation strength.

3.3 Climatic controls on precipitation isotope composition

This study performed a seasonal correlation analysis between precipitation isotopes (δ^2H, $\delta^{18}O$, d-excess, and $\Delta'^{17}O$) and meteorological parameters (air temperature, relative humidity, precipitation amount) (Fig. 5). The overall monthly averages across the study period revealed a significant correlation between meteorological variables and isotopes only for d-excess. This suggests that variations in $\delta^{18}O$ and $\Delta'^{17}O$ are governed by different meteorological influences that vary with season. In contrast, d-excess consistently exhibited significant negative correlations with relative humidity, temperature, and precipitation. These relationships likely reflect a combination of processes acting at different stages of the hydrological cycle. At the moisture source, lower relative humidity, often associated with cooler conditions, enhances kinetic fractionation during evaporation, leading to higher d-excess values (Merlivat and Jouzel, 1979; Uemura et al., 2008). During atmospheric transport and precipitation formation, local meteorological conditions, such as higher temperatures and lower humidity, may promote sub-

cloud re-evaporation and mixing between moist and dry air masses, thereby modifying and potentially reducing the original d-excess signal (Steen-Larsen et al., 2014). The negative correlation with precipitation may reflect the amount effect, but is better interpreted as a result of multiple interacting meteorological factors, such as variations in temperature, relative humidity, air-mass trajectories, precipitation intensity, and microphysical processes within clouds, that together influence the isotopic composition of precipitation (Holmes et al., 2024).

In spring, strong positive correlations were observed between $\delta^{18}O$ values and both temperature and precipitation ($r = 0.49$ and 0.53, respectively; $n = 10$ in each case). This indicates a significant temperature effect during spring due to relatively dry conditions and intermittent precipitation. The d-excess also displayed strong negative correlations with temperature during this period, providing insights into moisture sources and isotopic fractionation during precipitation (Uemura et al., 2008). During summer, $\delta^{18}O$ values were significantly negatively correlated with precipitation amount ($r = –0.44$, $n = 14$), reflecting the amount effect characteristic of monsoon climates. The relatively low $\delta^{18}O$ values during summer primarily result from prolonged monsoon precipitation and successive rainout within moisture-rich air masses of marine origin. In autumn, the monthly mean $\delta^{18}O$ was also strongly negatively correlated with precipitation amount ($r = –0.55$, $n = 10$), mainly due to frequent heavy rainfall events associated with typhoons or tropical cyclones, which are most common during this season. Although there were no direct passages of typhoons at the study site during the study period, substantial precipitation events influenced by typhoons were frequently observed. The strong correlations observed between d-excess and meteorological variables likely reflect moisture supply from nearby oceanic areas influenced by migratory high-pressure systems. In winter, d-excess and $\Delta'^{17}O$ showed negative correlations with temperature and precipitation amount, suggesting that these relationships reflect an integrated influence of moisture source conditions, atmospheric transport, and precipitation processes, rather than a direct response to evaporation conditions at the moisture source alone.

Overall, seasonal variations in precipitation isotopes across the Korean Peninsula reflect the combined influence of local meteorological conditions and synoptic-scale circulation patterns that control moisture source regions and precipitation mechanisms (Dansgaard, 1964; Ha et al., 2012; Huang et al., 2007; Lee et al., 2013). In particular, monsoon-driven moisture transport dominates summer isotopic depletion, while cold, dry continental air masses during winter exert an important control on isotopic composition, consistent with previous observations in East Asia (Kim et al., 2019; Lee et al., 2003). This seasonal variation underscores the role of changing moisture origins and precipitation mechanisms in modulating the stable isotope composition of precipitation across the Korean Peninsula.

3.4 Interpreting seasonal decoupling of $\Delta'^{17}O$ and d-excess

Variations in the $\Delta'^{17}O$ and d-excess of meteoric water are primarily governed by kinetic fractionation, making them reliable indicators of relative humidity at the moisture source (Barkan and Luz, 2007; Landais et al., 2010; Pfahl and Sodemann, 2014; Uemura et al., 2008). However, when measured in precipitation, these isotope indices may also reflect complex post-

evaporation processes such as continental recycling, partial re-evaporation within clouds, and sub-cloud raindrop evaporation (Landais et al., 2010; Li et al., 2015; Tian et al., 2018; Xia et al., 2023). These additional factors complicate the interpretation of seasonal isotopic variability in precipitation (Aron et al., 2023; Chen et al., 2023).

During spring, summer, and autumn, no statistically significant correlation was observed between Δ′17O and δ18O, likely because monthly precipitation values represent an integrated signal of multiple source-related and post-condensation processes rather than a simple linear relationship. In contrast, $\Delta'^{17}O$ showed a weak positive correlation with d-excess (Fig. 6). These tendencies are broadly consistent with theoretical expectations under non-steady-state oceanic evaporation at the moisture source, where kinetic fractionation induces a simultaneous increase in $\Delta'^{17}O$ and d-excess and a depletion in $\delta^{18}O$ and similar isotopic trends can also arise during sub-cloud rain re-evaporation (Li et al., 2015). The slopes observed between $\Delta'^{17}O$ and d-excess fall within the range of 0.7–2.0 per meg per ‰, which aligns with results from conceptual models and field-based estimates in regions influenced by oceanic moisture (Landais et al., 2010; Li et al., 2015). These observations suggest that, in non-winter seasons, kinetic processes acting during oceanic evaporation and subsequent sub-cloud re-evaporation of precipitation exert a dominant influence on isotopic composition. In contrast, in winter precipitation, no statistically significant correlation was observed between $\Delta'^{17}O$ and either $\delta^{18}O$ or d-excess. While the d-excess range remained relatively narrow in winter, $\Delta'^{17}O$ values showed a larger dispersion in this season (Fig. 3). This variability likely reflects multiple processes operating simultaneously under cold, dry atmospheric conditions. First, $\Delta'^{17}O$ is inherently more sensitive to water vapor mixing and nonequilibrium effects than d-excess, and may therefore decouple from $\delta^{18}O$-based processes under reduced surface moisture recycling (Li et al., 2015; Xia et al., 2023). Second, part of the enhanced winter $\Delta'^{17}O$ variability may also arise from ice–vapor equilibrium fractionation during snow formation, which affects $\Delta'^{17}O$ and d-excess differently from liquid-phase condensation (Jouzel and Merlivat,1984; Landais et al., 2012). Under such mixed-phase conditions, equilibrium enrichment associated with ice deposition can increase $\Delta'^{17}O$ while kinetic effects during water vapor transport or re-evaporation act in the opposite direction, producing the wide isotopic dispersion observed in winter samples. Taken together, these results indicate that winter isotopic variability in precipitation is governed not only by mid-tropospheric water vapor mixing and heterogeneous moisture sources but also by ice-phase fractionation processes that accompany snow formation, which are difficult to isolate in biweekly integrated samples.

During spring, summer, and autumn, $\Delta'^{17}O$ was negatively correlated with $\delta^{18}O$ and positively correlated with d-excess. These relationships reflect kinetic fractionation processes associated with evaporation and sub-cloud re-evaporation, with $\Delta'^{17}O$–d-excess slopes (0.7–2.0 per meg per ‰) consistent with previous modeling and observational studies (Landais et al., 2010; Li et al., 2015). Overall, these findings demonstrate the utility of $\Delta'^{17}O$, alongside $\delta^{18}O$ and d-excess, in disentangling the effects of evaporation, recycling, and mixing on precipitation isotopes across seasons.

3.5 Seasonal Comparison of Precipitation Isotope Trends: Observations vs. IsoGSM Model

Monthly mean precipitation δ^2H, $\delta^{18}O$ and d-excess from this study are compared with simulations from the isotope-enabled Global Spectral Model (IsoGSM) (Figure 7). IsoGSM simulates stable water isotopes within the atmospheric hydrological cycle and has been widely used to investigate large-scale isotope variability (Yoshimura et al., 2008). The model has been widely used to investigate the climatology and variability of precipitation isotopes and to evaluate isotope-enabled process representations in global models (Farlin et al., 2013; Kathayat et al., 2021; Kim et al., 2019; Tada et al., 2021). Both datasets reproduce the same broad seasonal patterns, with isotopically depleted summer precipitation and enriched winter values. However, some systematic differences are apparent. The IsoGSM outputs are slightly more depleted in δ^2H and $\delta^{18}O$, especially during late autumn and winter, and show a reduce amplitude of d-excess variability relative to the observations. These discrepancies likely reflect known limitations of isotope-enabled GCMs in representing kinetic fractionation processes and moisture recycling dynamics, particularly during cold-season conditions (Pfahl and Sodemann, 2014; Risi et al., 2008). While the IsoGSM captures the overall phasing of the seasonal isotope cycle, it tends to underestimate the amplitude of d-excess fluctuations, which are strongly influenced by sub-cloud evaporation, boundary-layer humidity, and re-evaporation of falling raindrops. In contrast, the observed dataset shows pronounced intra-annual variability in d-excess (approximately 5–20‰), especially outside the winter season, highlighting processes that are only partially represented in the model framework.

It is important to note that this comparison is intended as an illustrative example of how the precipitation isotope dataset can be used to benchmark model outputs rather than as a full-scale model evaluation. The observed model–data demonstrate how high-temporal-resolution isotope measurements can help identify the physical processes that requiring improved parameterization in isotope-enabled models, such as cloud–precipitation interactions, moisture-source tracking, and convective transport. Moreover, future model–data comparisons incorporating triple oxygen isotope measurements ($\Delta'^{17}O$) may provide additional constraints on non-equilibrium and mixing effects that are difficult to isolate using $\delta^{18}O$ and d-excess alone (Luz and Barkan, 2010; Landais et al., 2008), highlighting the potential of the present dataset as a regional benchmark for improving isotope-enabled model parameterizations.

4 Conclusions

This study examined 130 precipitation samples collected in Seoul between 2016 and 2020 to quantify seasonal variability in δ^2H, $\delta^{18}O$, $\delta^{17}O$, d-excess, and $\Delta'^{17}O$ and clarify how these isotope tracers respond to local meteorological conditions. $\delta^{17}O$, $\delta^{18}O$, and δ^2H followed a pronounced sinusoidal seasonal cycle, being most depleted during winter, becoming gradually enriched in spring, and sharply declining during the summer monsoon due to the amount effect. d-excess was highest in winter and lowest in summer, reflecting its sensitivity to non-equilibrium evaporation and relative humidity at the moisture source. Meanwhile, $\Delta'^{17}O$ exhibited a similar seasonal cycle with a reduced amplitude, indicating that, although both $\Delta'^{17}O$ and d-excess are influenced by large-scale circulation and water vapor transport, $\Delta'^{17}O$ is relatively more sensitive to these processes.

The calculated Local Meteoric Water Line ($\delta^2H=7.79\pm0.35\cdot\delta^{18}O+10.2\pm2.7$) closely resembles the Global Meteoric Water Line, but with a higher winter intercept, suggesting enhanced ice-phase fractionation and the influence of dry continental air masses. The $\delta^{17}O$–$\delta^{18}O$ relationship indicated equilibrium fractionation dominates the isotope system during the non-winter seasons, whereas the steeper slope observed in winter reflects an increased contribution from kinetic fractionation under low humidity conditions.

The comparison of the seasonal behavior of $\delta^{18}O$, d-excess, and $\Delta'^{17}O$ revealed distinct tracer-specific responses. During spring, summer, and autumn, $\Delta'^{17}O$ was negatively correlated with $\delta^{18}O$ and positively correlated with d-excess, consistent with theoretical expectations for non-steady-state evaporation. The slope between $\Delta'^{17}O$ and d-excess ranged from 0.7 to 2.0 per meg per ‰, aligning with conceptual models and empirical results from ocean-influenced regions, while also failing within the range of slopes associated with sub-cloud rain re-evaporation. In contrast, in winter, no statistically significant correlation was observed between $\Delta'^{17}O$ and either $\delta^{17}O$ or d-excess, while $\Delta'^{17}O$ displayed greater dispersion to compared to other season. This decoupling likely reflects the heightened sensitivity of $\Delta^{17}O$ to mid-tropospheric water vapor mixing and contributions from diverse moisture sources, rather than surface evaporation alone. These findings underscore the utility of $\Delta'^{17}O$ as a diagnostic tracer of atmospheric mixing and moisture transport, especially in cold seasons.

By integrating $\delta^{18}O$, d-excess, and $\Delta'^{17}O$, this study provides a more comprehensive understanding of seasonal hydrological processes than would be possible using any of these tracers alone. The results highlight key controls on isotopic variability in the East Asian monsoon system, particularly during winter, when interactions between continental and marine air masses become dominant. This dataset serves as a valuable benchmark for interpreting modern hydroclimatic dynamics and offers a foundation for evaluating isotope-enabled climate models. Beyond contemporary climate diagnostics, the integrated use of $\Delta'^{17}O$ and d-excess also holds implications for interpreting isotope records in subsurface hydrological archives. These tracers may enable enhanced reconstructions of past climatic conditions from speleothems or glacier ice and improve the understanding of groundwater recharge processes in monsoon-influenced regions. As such, this work bridges modern atmospheric processes with paleoclimate interpretations and supports future hydroclimate modeling and water resource management across East Asia.

5 Data availability

All precipitation isotope data generated and analyzed in this study are publicly available through the PANGAEA data repository. The dataset includes precipitation-weighted monthly mean values of δ^2H, $\delta^{18}O$, $\delta^{17}O$, d-excess, and $\Delta'^{17}O$ for Seoul, South Korea, covering the period from 2016 to 2020. The data can be accessed at: Kim, Songyi; Han, Yeongcheol; Jung, Hyejung; Lee, Jeonghoon (2025): Monthly means of triple isotopic compositions of precipitation in Seoul (2016–2020)[dataset]. PANGAEA, https://doi.org/10.1594/PANGAEA.983390.

Author contributions. This study was conceptualized by JL. Data were collected and analyzed by SK, YH and HJ. The paper was written by SK and JL, with contributions from all authors.

Acknowledgements. This research was supported by the Korea Polar Research Institute grant (PE25100) and the National Research Foundation of Korea grant funded by the Korean Government (NRF2022R1A2C3007047). This study was partially supported by Korea Environment Industry & Technology Institute (KEITI) through Aquatic Ecosystem Conservation Research Program, funded by the Korea Ministry of Environment (MOE) (RS-2024-00332851).

References

Aggarwal, P. K., Araguás-Araguás, L. J., Groening, M., Kulkarni, K. M., Kurttas, T., Newman, B. D., and Vitvar, T.: Global Hydrological Isotope Data and Data Networks, in: Isoscapes: Understanding movement, pattern, and process on Earth through isotope mapping, edited by: West, J. B., Bowen, G. J., Dawson, T. E., and Tu, K. P., Springer Netherlands, Dordrecht, 33–50, https://doi.org/10.1007/978-90-481-3354-3_2, 2010.

Angert, A., Cappa, C. D., and DePaolo, D. J.: Kinetic ^{17}O effects in the hydrologic cycle: Indirect evidence and implications, Geochimica et Cosmochimica Acta, 68, 3487–3495, https://doi.org/10.1016/j.gca.2004.02.010, 2004.

Araguás-Araguás, L., Froehlich, K., and Rozanski, K.: Stable isotope composition of precipitation over southeast Asia, J. Geophys. Res., 103, 28721–28742, https://doi.org/10.1029/98JD02582, 1998.

Aron, P. G., Li, S., Brooks, J. R., Welker, J. M., and Levin, N. E.: Seasonal Variations in Triple Oxygen Isotope Ratios of Precipitation in the Western and Central United States, Paleoceanography and Paleoclimatology, 38, e2022PA004458, https://doi.org/10.1029/2022PA004458, 2023.

Barkan, E. and Luz, B.: High precision measurements of $^{17}O/^{16}O$ and $^{18}O/^{16}O$ ratios in H_2O, Rapid Comm Mass Spectrometry, 19, 3737–3742, https://doi.org/10.1002/rcm.2250, 2005.

Barkan, E. and Luz, B.: Diffusivity fractionations of HO/HO and HO/HO in air and their implications for isotope hydrology, Rapid Comm Mass Spectrometry, 21, 2999–3005, https://doi.org/10.1002/rcm.3180, 2007.

Benetti, M., Reverdin, G., Pierre, C., Merlivat, L., Risi, C., Steen-Larsen, H. C., and Vimeux, F.: Deuterium excess in marine water vapor: Dependency on relative humidity and surface wind speed during evaporation, JGR Atmospheres, 119, 584–593, https://doi.org/10.1002/2013JD020535, 2014.

Bowen, G. J., Putman, A., Brooks, J. R., Bowling, D. R., Oerter, E. J., and Good, S. P.: Inferring the source of evaporated waters using stable H and O isotopes, Oecologia, 187, 1025–1039, https://doi.org/10.1007/s00442-018-4192-5, 2018.

Cappa, C. D., Hendricks, M. B., DePaolo, D. J., and Cohen, R. C.: Isotopic fractionation of water during evaporation, J. Geophys. Res., 108, 2003JD003597, https://doi.org/10.1029/2003JD003597, 2003.

Chen, J., Chen, J., Zhang, X. J., Peng, P., and Risi, C.: A century and a half precipitation oxygen isoscape for China generated using data fusion and bias correction, Sci Data, 10, 185, https://doi.org/10.1038/s41597-023-02095-1, 2023.

Conroy, J. L., Noone, D., Cobb, K. M., Moerman, J. W., and Konecky, B. L.: Paired stable isotopologues in precipitation and vapor: A case study of the amount effect within western tropical Pacific storms, JGR Atmospheres, 121, 3290–3303, https://doi.org/10.1002/2015JD023844, 2016.

Craig, H.: Isotopic Variations in Meteoric Waters, Science, 133, 1702–1703, https://doi.org/10.1126/science.133.3465.1702, 1961.

Craig, H. and Gordon, L. I.: Deuterium and oxygen 18 variations m the ocean and the marine atmosphere, in: Stable Isotopes in Oceanographic Studies and Paleotemperatures, Pisa, Spoleto, Italy, 9–130, 1965.

Dansgaard, W.: Stable isotopes in precipitation, Tellus, 16, 436–468, https://doi.org/10.1111/j.2153-3490.1964.tb00181.x, 1964.

Farlin, J., Lai, C.-T., and Yoshimura, K.: Influence of synoptic weather events on the isotopic composition of atmospheric moisture in a coastal city of the western United States: Synoptic Controls on Isotope Ratios of Atmospheric Moisture, Water Resour. Res., 49, 3685–3696, https://doi.org/10.1002/wrcr.20305, 2013.

Gat, J. R.: Oxygen and hydrogen isotopes in the hydrologic cycle, *Annu. Rev. Earth Planet. Sci.*, **24**, 225–262, https://doi.org/10.1146/annurev.earth.24.1.225, 1996.

Gupta, P., Noone, D., Galewsky, J., Sweeney, C., and Vaughn, B. H.: Demonstration of high-precision continuous measurements of water vapor isotopologues in laboratory and remote field deployments using wavelength-scanned cavity ring-down spectroscopy (WS-CRDS) technology, Rapid Comm Mass Spectrometry, 23, 2534–2542, https://doi.org/10.1002/rcm.4100, 2009.

Ha, K.-J., Heo, K.-Y., Lee, S.-S., Yun, K.-S., and Jhun, J.-G.: Variability in the East Asian Monsoon: a review, Meteorological Applications, 19, 200–215, https://doi.org/10.1002/met.1320, 2012.

Holmes, J., Jourdan ,Anne-Lise, and and Darling, W. G.: Stable-isotope variability in daily precipitation: insights from a low-cost collector in SE England, Isotopes in Environmental and Health Studies, 60, 596–614, https://doi.org/10.1080/10256016.2024.2402730, 2024.

Huang, R., Chen, J., and Huang, G.: Characteristics and variations of the East Asian monsoon system and its impacts on climate disasters in China, Adv. Atmos. Sci., 24, 993–1023, https://doi.org/10.1007/s00376-007-0993-x, 2007.

Jouzel, J., Alley, R. B., Cuffey, K. M., Dansgaard, W., Grootes, P., Hoffmann, G., Johnsen, S. J., Koster, R. D., Peel, D., Shuman, C. A., Stievenard, M., Stuiver, M., and White, J.: Validity of the temperature reconstruction from water isotopes in ice cores, J. Geophys. Res., 102, 26471–26487, https://doi.org/10.1029/97JC01283, 1997.

Kathayat, G., Sinha, A., Tanoue, M., Yoshimura, K., Li, H., Zhang, H., and Cheng, H.: Interannual oxygen isotope variability in Indian summer monsoon precipitation reflects changes in moisture sources, Commun Earth Environ, 2, 1–10, https://doi.org/10.1038/s43247-021-00165-z, 2021.

Kim, S., Han, Y., Hur, S. D., Yoshimura, K., and Lee, J.: Relating Moisture Transport to Stable Water Vapor Isotopic Variations of Ambient Wintertime along the Western Coast of Korea, Atmosphere, 10, 806, https://doi.org/10.3390/atmos10120806, 2019.

Kim, S., Han, C., Moon, J., Han, Y., Hur, S. D., and Lee, J.: An optimal strategy for determining triple oxygen isotope ratios in natural water using a commercial cavity ring-down spectrometer, Geosci J, 26, 637–647, https://doi.org/10.1007/s12303-022-0009-y, 2022.

Korea Meteorological Administration (KMA): Meteorological observation data for Seoul station (hourly), available at: https://www.weather.go.kr, last access: 15 March 2024.

Landais, A., Barkan, E., and Luz, B.: Record of $\delta^{18}O$ and ^{17}O-excess in ice from Vostok Antarctica during the last 150,000 years, Geophysical Research Letters, 35, 2007GL032096, https://doi.org/10.1029/2007GL032096, 2008.

Landais, A., Risi, C., Bony, S., Vimeux, F., Descroix, L., Falourd, S., and Bouygues, A.: Combined measurements of ^{17}Oexcess and d-excess in African monsoon precipitation: Implications for evaluating convective parameterizations, Earth and Planetary Science Letters, 298, 104–112, https://doi.org/10.1016/j.epsl.2010.07.033, 2010.

Landais, A., Ekaykin, A., Barkan, E., Winkler, R., and Luz, B.: Seasonal variations of ^{17}O-excess and d-excess in snow precipitation at Vostok station, East Antarctica, J. Glaciol., 58, 725–733, https://doi.org/10.3189/2012JoG11J237, 2012.

Lee, J., Worden, J., Koh, D.-C., Yoshimura, K., and Lee, J.-E.: A seasonality of δD of water vapor (850-500 hPa) observed from space over Jeju Island, Korea, Geosci J, 17, 87–95, https://doi.org/10.1007/s12303-013-0003-5, 2013.

Lee, K., Grundstein, A., Wenner, D., Choi, M., Woo, N., and Lee, D.: Climatic controls on the stable isotopic composition of precipitation in Northeast Asia, Clim. Res., 23, 137–148, https://doi.org/10.3354/cr023137, 2003.

Lee, K.-S. and Kim, Y.: Determining the seasonality of groundwater recharge using water isotopes: a case study from the upper North Han River basin, Korea, Environ Geol, 52, 853–859, https://doi.org/10.1007/s00254-006-0527-3, 2007.

Lee, K.-S., Kim, J.-M., Lee, D.-R., Kim, Y., and Lee, D.: Analysis of water movement through an unsaturated soil zone in Jeju Island, Korea using stable oxygen and hydrogen isotopes, Journal of Hydrology, 345, 199–211, https://doi.org/10.1016/j.jhydrol.2007.08.006, 2007.

Li, S., Levin, N. E., and Chesson, L. A.: Continental scale variation in ^{17}O-excess of meteoric waters in the United States, Geochimica et Cosmochimica Acta, 164, 110–126, https://doi.org/10.1016/j.gca.2015.04.047, 2015.

Lim, C., Lee, I., Lee, S.-M., Yu, J.-Y., and Kaufman, A. J.: Sulfur, oxygen, and hydrogen isotope compositions of precipitation in Seoul, South Korea, Geochem. J., 46, 443–457, https://doi.org/10.2343/geochemj.1.0173, 2012.

Luz, B. and Barkan, E.: Variations of $^{17}O/^{16}O$ and $^{18}O/^{16}O$ in meteoric waters, Geochimica et Cosmochimica Acta, 74, 6276–6286, https://doi.org/10.1016/j.gca.2010.08.016, 2010.

Luz, B. and Barkan, E.: The isotopic composition of atmospheric oxygen: ISOTOPIC COMPOSITION OF AIR OXYGEN, Global Biogeochem. Cycles, 25, 1–14, https://doi.org/10.1029/2010GB003883, 2011.

Majoube, M.: Fractionnement en oxygène 18 et en deutérium entre l'eau et sa vapeur, Journal de Chimie Physique, 68, 1423–1436, https://doi.org/10.1051/jcp/1971681423, 1971.

Masson-Delmotte, V., Panmao, Z., Anna, P., Sarah, L. C., Clotilde, P., Yang, C., Leah, G., Melissa, I. G., J.B. Robin, M., Sophie, B., Mengtian, H., Ozge, Y., Rong, Y., Baiquan, Z., Elisabeth, L., Thomas, K. M., Tim, W., Katherine, L., and Nada: Climate Change 2021 – The Physical Science Basis: Working Group I Contribution to the Sixth Assessment Report of the

Intergovernmental Panel on Climate Change, 1st ed., Cambridge University Press, https://doi.org/10.1017/9781009157896, 2021.

Merlivat, L. and Jouzel, J.: Global climatic interpretation of the deuterium-oxygen 18 relationship for precipitation, J. Geophys. Res., 84, 5029–5033, https://doi.org/10.1029/JC084iC08p05029, 1979.

Pfahl, S. and Sodemann, H.: What controls deuterium excess in global precipitation?, Clim. Past, 10, 771–781, https://doi.org/10.5194/cp-10-771-2014, 2014.

Shin, Y., Kim, T., Moon, S., Yun, S.-T., Moon, D., Han, H., and Kang, K.: A Study on the Recharge Characteristics of Groundwater in the Jeju Samdasoo Watershed Using Stable Water Isotope Data, Journal of Soil and Groundwater Environment, 26, 25–36, https://doi.org/10.7857/JSGE.2021.26.3.025, 2021.

Steen-Larsen, H. C., Sveinbjörnsdottir, A. E., Peters, A. J., Masson-Delmotte, V., Guishard, M. P., Hsiao, G., Jouzel, J., Noone, D., Warren, J. K., and White, J. W. C.: Climatic controls on water vapor deuterium excess in the marine boundary layer of the North Atlantic based on 500 days of in situ, continuous measurements, Atmos. Chem. Phys., 14, 7741–7756, https://doi.org/10.5194/acp-14-7741-2014, 2014.

Tada, M., Yoshimura, K., and Toride, K.: Improving weather forecasting by assimilation of water vapor isotopes, Sci Rep, 11, 18067, https://doi.org/10.1038/s41598-021-97476-0, 2021.

Tian, C., Wang, L., Kaseke, K. F., and Bird, B. W.: Stable isotope compositions (δ^2H, δ^{18}O and δ^{17}O) of rainfall and snowfall in the central United States, Sci Rep, 8, 6712, https://doi.org/10.1038/s41598-018-25102-7, 2018.

Trenberth, K.: Changes in precipitation with climate change, Clim. Res., 47, 123–138, https://doi.org/10.3354/cr00953, 2011.

Uemura, R., Matsui, Y., Yoshimura, K., Motoyama, H., and Yoshida, N.: Evidence of deuterium excess in water vapor as an indicator of ocean surface conditions, J. Geophys. Res., 113, 2008JD010209, https://doi.org/10.1029/2008JD010209, 2008.

Winkler, R., Landais, A., Sodemann, H., Dümbgen, L., Prié, F., Masson-Delmotte, V., Stenni, B., and Jouzel, J.: Deglaciation records of ^{17}O-excess in East Antarctica: reliable reconstruction of oceanic normalized relative humidity from coastal sites, Clim. Past, 8, 1–16, https://doi.org/10.5194/cp-8-1-2012, 2012.

Xia, Z., Surma, J., and Winnick, M. J.: The response and sensitivity of deuterium and ^{17}O excess parameters in precipitation to hydroclimate processes, Earth-Science Reviews, 242, 104432, https://doi.org/10.1016/j.earscirev.2023.104432, 2023.

Yoon, Y. Y. and Koh, D. C.: Tritium and stable isotope content variation in precipitation at Hongseung: West Korea Region, J Radioanal Nucl Chem, 330, 413–417, https://doi.org/10.1007/s10967-021-07955-x, 2021.

Yoshimura, K., Kanamitsu, M., Noone, D., and Oki, T.: Historical isotope simulation using Reanalysis atmospheric data, J. Geophys. Res., 113, 2008JD010074, https://doi.org/10.1029/2008JD010074, 2008.

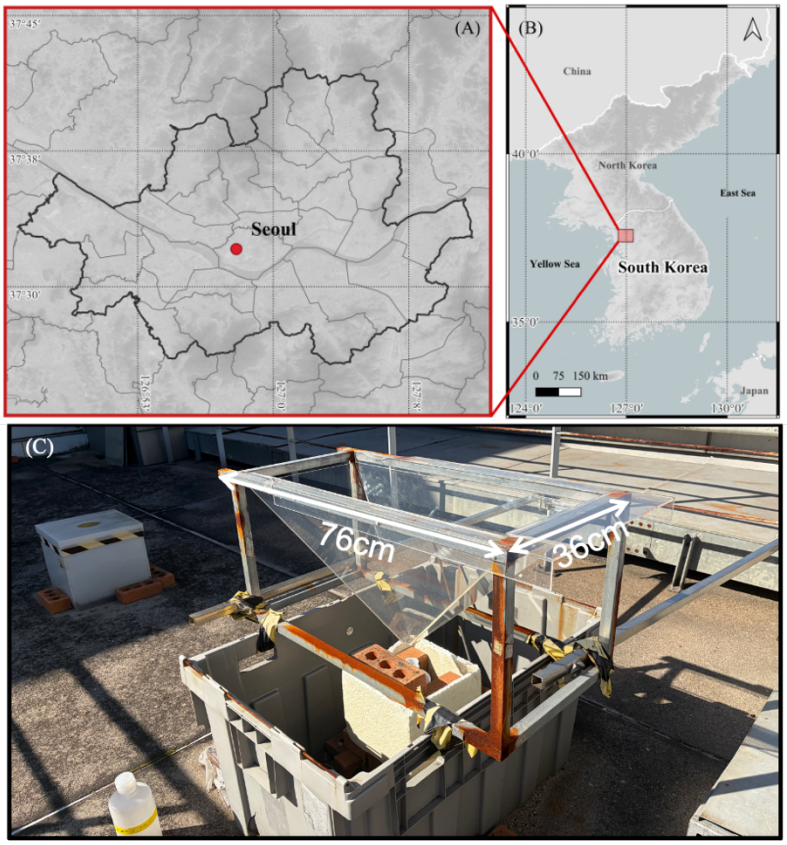

Figure 1: (A) A map showing the location of South Korea within East Asia. (B) An enlarged map highlighting the study site (red dot) in Seoul, South Korea, with administrative boundaries for surrounding regions. (C) The precipitation sampling device that was installed at the study site, designed to minimize post-collection evaporation.

500

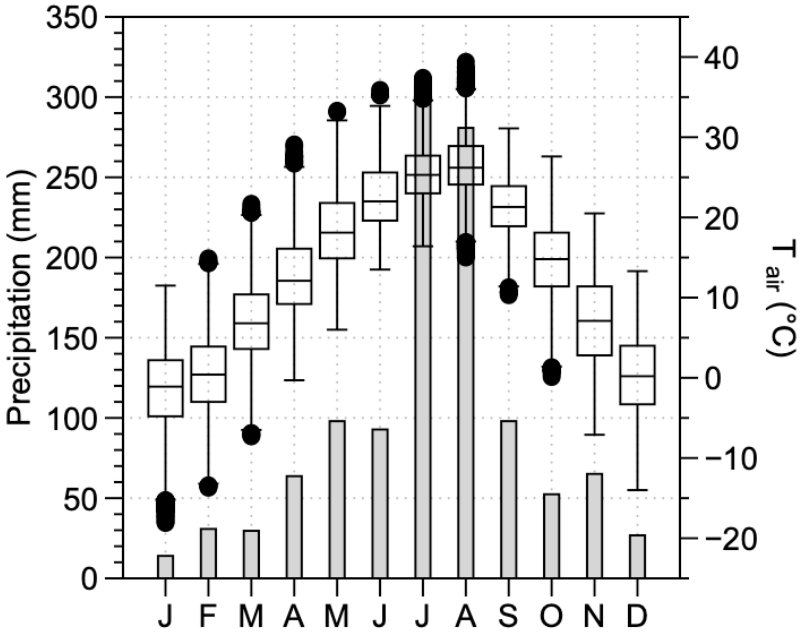

Figure 2: The average monthly precipitation amount (grey bars) and average monthly temperature (black-lined boxes) for the city of Seoul, based on meteorological data provided by the Korea Meteorological Administration (available at: https://www.weather.go.kr/w/index.do).

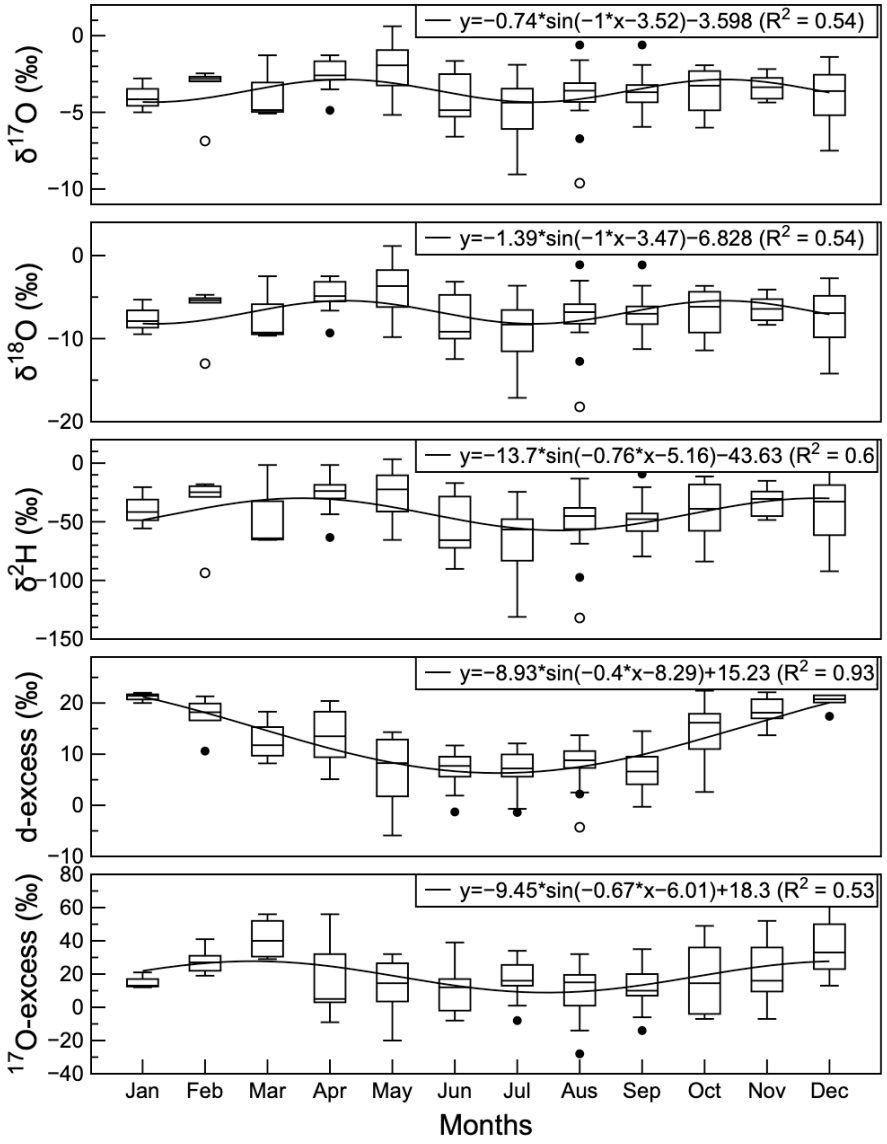

505

Figure 3: The monthly average values of the observed isotopic tracers. From top to bottom: $\delta^{17}O$, $\delta^{18}O$, $\delta^{2}H$, deuterium excess (d-excess), and ^{17}O-excess.

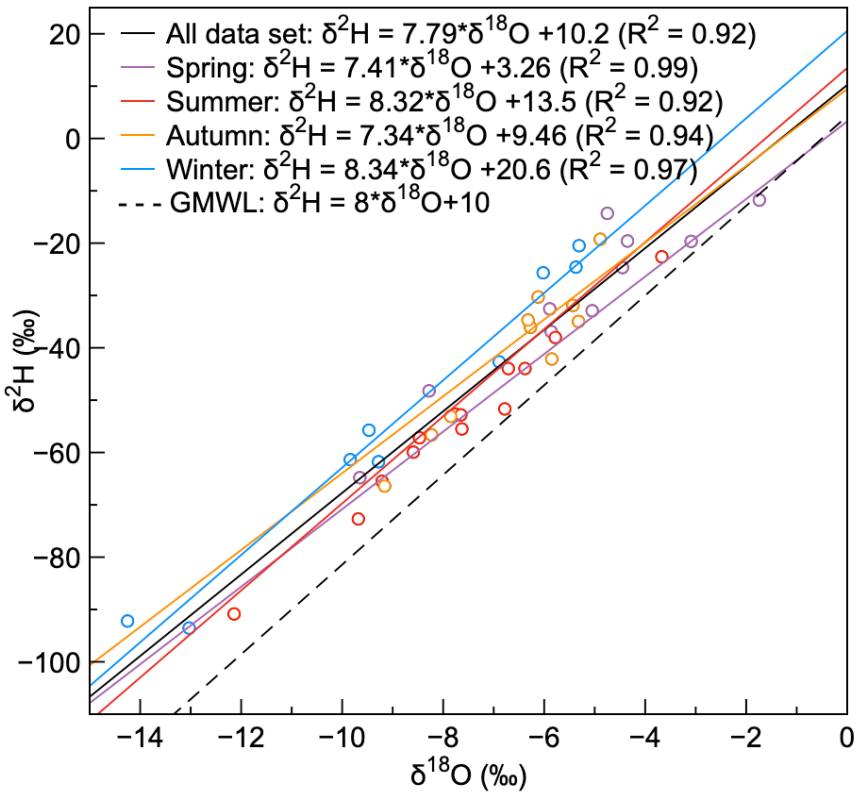

Figure 4: The values of isotopic tracers by season, with regression lines for each. The black regression line represents the aggregated data for the entire year, which served as a baseline for seasonal variations. Red points and their regression line indicate the summer trend. Blue points with the corresponding regression line depict the winter values. The black dash line denotes the Global Meteoric Water Line (GMWL).

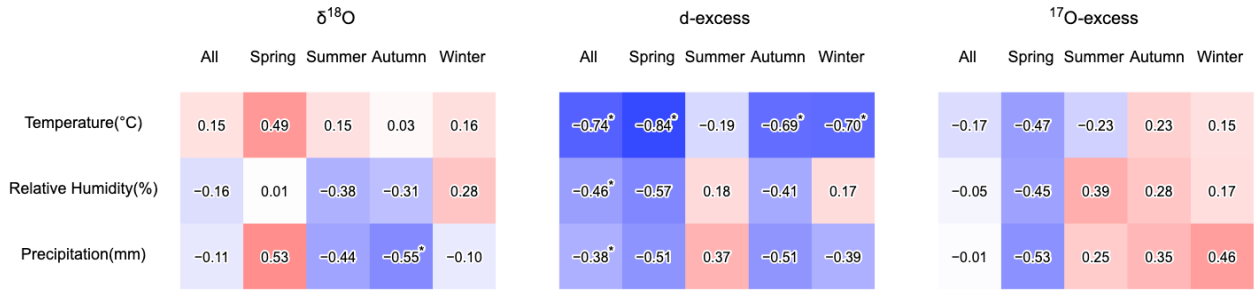

515

Figure 5: Correlations between precipitation-weighted mean monthly precipitation isotopes ($\delta^{18}O$, d-excess, and ^{17}O-excess) and the precipitation-weighted mean meteorological variables (air temperature, relative humidity) and total precipitation amount during the study period.

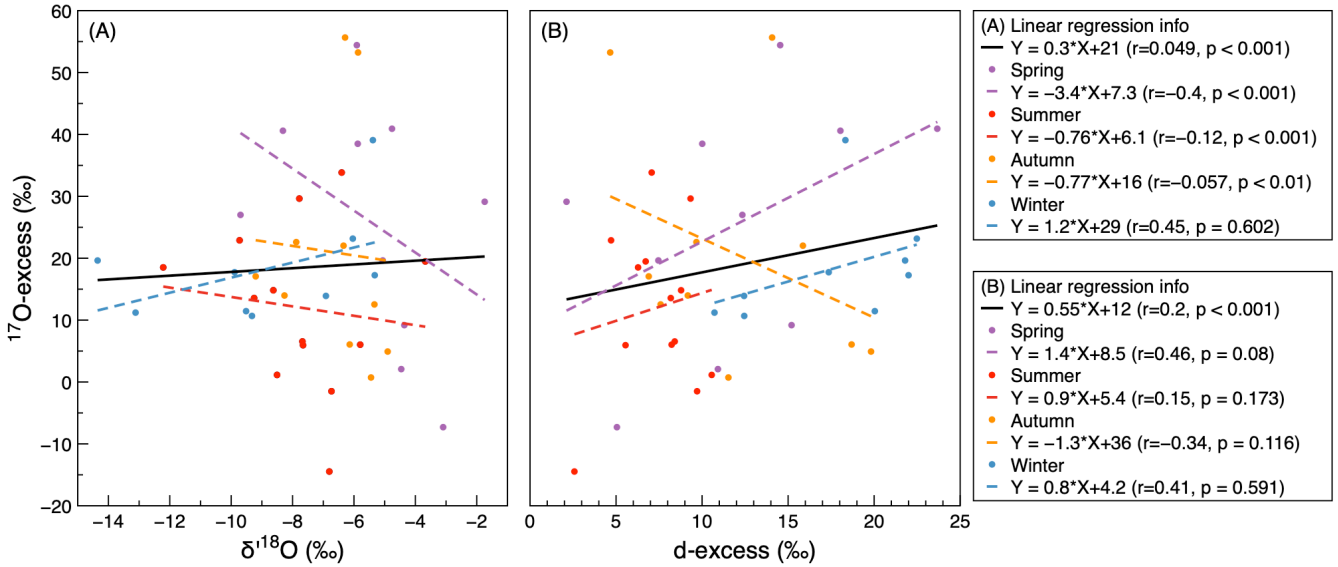

Figure 6: The seasonal relationships between ^{17}O-excess and (A) δ^{18}O and (B) d-excess. Each marker represents a monthly weighted mean sample, color-coded by season (violet = spring; red = summer; orange = autumn; blue = winter). The regression line for each season is shown as a dashed line in the corresponding color, while the solid black lines represent the regression for the entire dataset. The regression equations and Pearson correlation coefficients (r) are listed in the legends.

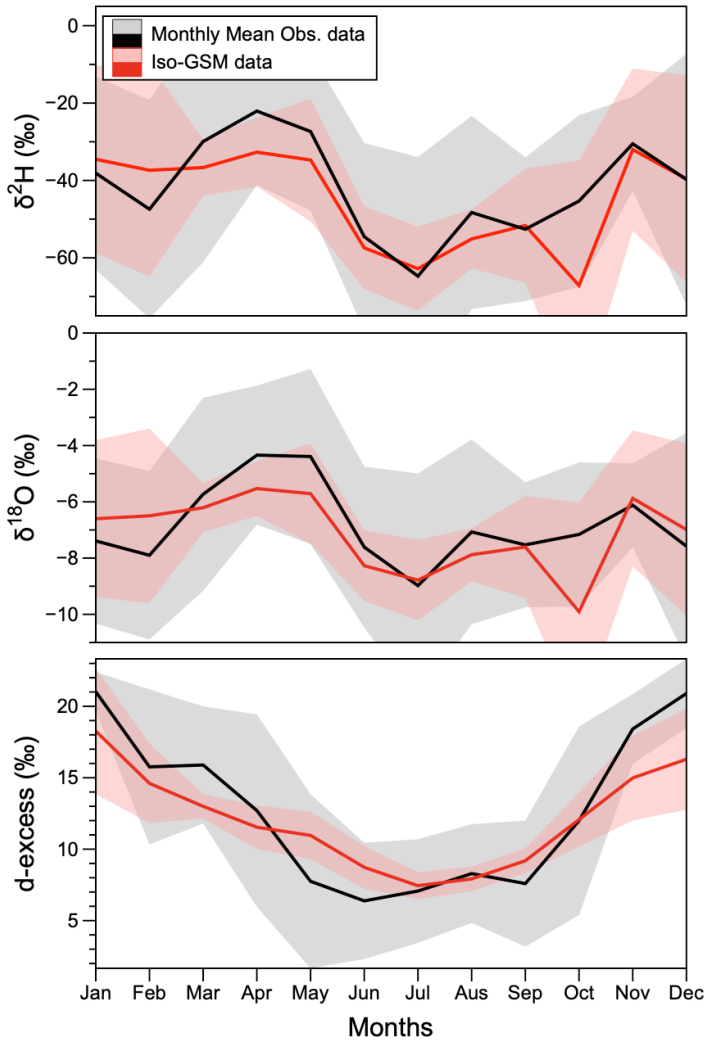

Figure 7: The monthly mean precipitation stable isotope values (δ^2H, $\delta^{18}O$, and d-excess) from observations (black solid line with gray shading) and Isotope-enabled Global Spectral Model (Iso-GSM) outputs (red solid line with pink shading). The shaded areas represent the uncertainty range of the monthly mean (±1 standard deviation), while the solid lines indicate the monthly average values.